MAGNETIC FIELD EFFECTS ON VISCOUS FINGERING OF A FERROFLUID IN AN ANISOTROPIC HELE–SHAW CELL

R. Ballou, P. Molho
Laboratoire Louis Néel, CNRS, BP 166, 38042 Grenoble Cedex 9, France
(molho@grenoble.cnrs.fr)

Introduction. When a viscous fluid is pushed into a more viscous one in a Hele–Shaw cell, the interface between the two fluids may become unstable, leading to fingering and ramified patterns [1]. Anisotropy can be introduced by engraving a grid in one plate of the cell [2], allowing one to obtain dendritic patterns. The use of a ferrofluid as one of the viscous fluid is a way to introduce magnetism in the problem, especially the magnetic field as a control parameter. Magnetic field effects on viscous fingering of ferrofluids have already been studied: in a rectangular Hele–Shaw cell, a magnetic field applied in the cell plane is stabilizing when parallel to the interface between the two fluids and destabilizing when normal to the interface [3]. A magnetic field perpendicular to the plane of a radial Hele–Shaw cell has the same destabilizing effect as the pressure [4]. We have studied the effect of a magnetic field, normal to and in the plane of anisotropic radial Hele–Shaw cells [5], to characterize the competing effects of hydrodynamics, magnetic field and dipolar energy, and anisotropy. Here we study more precisely the effect of a magnetic field normal to a radial anisotropic Hele–Shaw cell.

1. Experimental setup. The Hele–Shaw cells we used are composed of two plexiglas plates 5 mm thick, of diameter 50 mm, with an inter-plates spacing from 0.15 mm to 0.50 mm. Hexagonal or square anisotropy is introduced by engraving circular shaped lattice elements in the bottom plate, of diameter, depth and edge-to-edge distance of 0.50 mm. The ratio between the depth of the engraved elements b', and the cell thickness b, defines the effective anisotropy. Magnetic fields are produced by a device built with permanent magnets called "magnetic mangle" [6]. It allows us to apply fields up to 0.23 T, approximately homogeneous in a volume of about $2 \times 2 \times 2$ cm^3. Some experiments were performed in more homogeneous fields generated by an electromagnet. Both apparatuses show the same field effects. The ferrofluid was injected at the center of the cell, through a hole in the top plate, using a syringe pushed by hand, controlling qualitatively the pressure in a reproducible way. The magnetic fluid we used is based on cobalt ferrite dispersed in a 50/50 mixture of glycerol and water, of dynamical viscosity $\eta = 10$ mPa $\cdot$ s, immiscible with the silicone oils of dynamic viscosity ranging from 200 to 29100 mPa $\cdot$ s. The parameters of each experiment are given with the following notation: [cell thickness (mm), anisotropy type (-, sq, hex or sq*), dynamical viscosity η (mPa $\cdot$ s)]. sq* denotes a square lattice with a larger depth of the holes of 1.00 mm.

2. Experiments. When no magnetic field is applied, the ferrofluid behaves like an ordinary fluid and the experiments show the usually observed patterns: equilibrium shapes when the growth is very slow, circular or facetted in case of anisotropy (Fig. 1*a*); oriented fingers related to tip-splitting processes (Fig. 1*b*); dendrites on hexagonal grids (Fig. 1*c*).

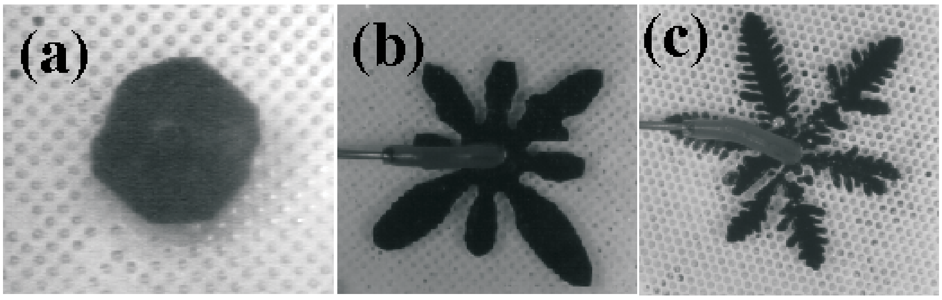

Fig. 1. Patterns corresponding to different growth regimes in anisotropic cells with no magnetic field. (*a*): facetted [0.30, sq*, 200]; (*b*): oriented fingers [0.20, sq, 1000]; (*c*): dendrites [0.20, hex, 29100].

When a magnetic field normal to the cell is applied, the ferrofluid gets magnetized and, in order to minimize dipolar energy, the holes of the engraved plate of the cell tend to be filled with the ferrofluid. This process is somehow analogous to the normal field instability in a thin film of ferrofluid. This tendency to fill the holes, combined with the viscous fingering process leads to different patterns, depending on the "growth regime".

When the field is applied on an already grown drop (Fig. 1*a*), the envelope is preserved and the obtained pattern is compact but "discrete" (Fig. 2*a*). When a slow injection is performed under the normal field, the holes are filled uniformly, but the shape of the envelope reveals the underlying anisotropy (Fig. 2*b*). When the injection is faster, the probability of filling the holes is not uniform and keeps a random character leading to a pattern reminiscent of DLA fractal aggregates (Fig. 2*c*). Finally, during a fast growth regime, the injected fluid follows only directions defined by the anisotropy and the filled holes reveal sharply the dendritic morphology (Fig. 2*d*).

This experimental sequence is described in term of slow and fast injection. In fact, the control parameters are not that straightforward. A way to change the growth regime is to change the viscosity, or the cell thickness, or the injection rate. A larger viscosity leads to a "faster" growth regime for the same injection rate. In the same way, a manner to change the anisotropy strength is to change the ratio between the hole depth and the thickness of the cell but this can also be achieved by changing the symmetry of the engraved grid: the hexagonal symmetry is more efficient that the square one to generate dendrites. The magnetic field intensity is another way to change the effective anisotropy (it has also an effect on the fingering itself). Changing the depth of the holes, or the field intensity allows to change from a regime of negligible anisotropy leading to a labyrinth, which minimizes energy, to a regime of holes filling, leading to discrete patterns.

Those patterns obtained by filling the engraved holes are interesting, since they are different from the usual viscous fingering and quite similar to an "experimental" DLA.

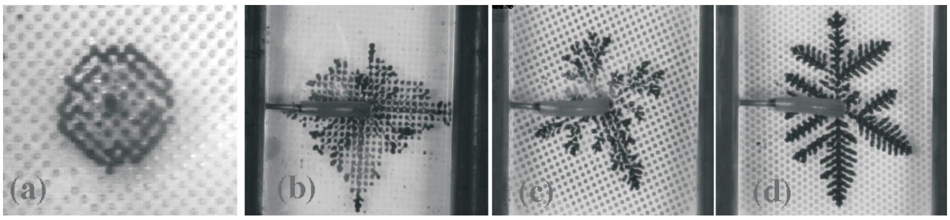

Fig. 2. Filling of the holes of anisotropic cells in the normal field. (*a*): [0.30, sq*, 200]; (*b*): [0.20, sq, 1000]; (*c*): [0.15, sq, 29100]; (*d*): [0.15, hex, 29100].

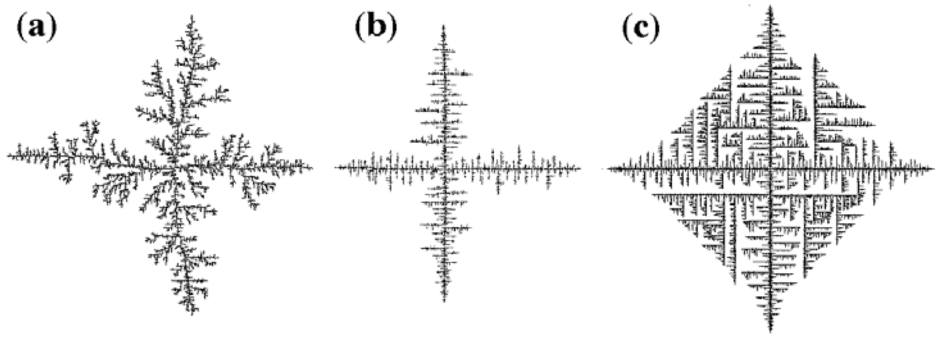

Fig. 3. Examples of numerical patterns. (*a*): typical DLA aggregate (14000 particles); (*b*): DLA with noise reduction (5000 particles, m=10); (*c*): modified DLA by a percentage of radial motion $c = 0.01$ and noise reduction $m = 40$ (24000 particles).

3. Numerical simulations. In order to have a better insight on the different regimes, we performed numerical simulations based on a DLA model [7]. This discrete model has been shown to be relevant to describe experiments like viscous fingering (see, for instance, [8, 9]). Usual DLA leads to a well known fractal pattern (Fig. 3*a*). Many modifications have been implemented in this model, both on the particle diffusion and on the sticking rules. In our case, we used mainly two additional parameters. The first one is a measure of noise reduction known to reveal the anisotropy resulting from the underlying lattice. This noise reduction consists in sticking a particle on the aggregate only when the possibility of sticking on the site was realized m times. The second parameter is a percentage of radial motion superimposed to diffusion. Instead of a probability 0.25 of choosing one direction on the square lattice, the probability is corrected by a projection on the 4 directions of a unit vector oriented toward the origin of the aggregate, multiplied by a coefficient c. Both parameters affect the anisotropy of the system.

The usual DLA aggregate (Fig. 3*a*) corresponds to the intermediate growth regime observed experimentally (Fig. 2*c*). Noise reduction has a striking effect, leading to sharply defined dendrites, even for small values of m (Fig. 3*b*). This pattern is somehow similar to the one obtained experimentally in the fast injection regime (Fig. 2*d*). When some radial motion is superimposed to the diffusion, the pattern becomes more isotropic, and when combined with noise reduction, leads to a pattern with an envelope reflecting the lattice symmetry. This is analogous to the slow injection regime pattern (Fig. 2*b*).

We also used a third parameter, which can account for surface tension: when a particle reaches the aggregate, it sticks with a given probability or keeps moving. This leads to more compact aggregates, and some characteristic width of the growing fingers could perhaps be defined. Such dense aggregate may account for the one presented in Fig. 2*a*.

4. Conclusion. In the experiments, the magnetic field reinforces the anisotropy, leading to different discrete morphologies when the growth regime is modified, for instance by changing the viscosity. DLA numerical simulations, where anisotropy can be introduced by an underlying lattice, and controlled by noise reduction and a motion of the particles more isotropic than in the case of a random walk, capture the essential of the observed patterns. Finally, by increasing the anisotropy in a somehow simple model like DLA, it is possible to generate patterns quite similar to the ones observed in our experiment. The way the anisotropy is controlled in the model is quite subtle, since the two parameters used act in a very different way: a percentage of radial motion leads to more isotropic patterns, while noise reduction increases the effect of the underlying lattice. Using more parameters (surface tension, other symmetries, off lattice DLA. . .) should allow to obtain more precisely the observed sequence of patterns.

Acknowledgments. The authors wish to thank Sophie Neveu for providing them with the ferrofluid and Wietze Herreman who was involved in the experiments.

REFERENCES

1. D. Bensimon *et al.* *Rev. Mod. Phys.*, vol. 58 (1986), p. 977.
2. E. Ben-Jacob *et al.* *Phys. Rev. Lett.*, vol. 55 (1985), p. 1315.
3. R.E. Rosensweig. *Ferrohydrodynamics* (Dover, Mineola, NY, 1997).
4. C. Flament *et al.* *Physics of Fluids*, vol. 10 (1998), p. 2464.
5. W. Herreman, P. Molho, S. Neveu. *J. Magn. Magn. Mater*, vol. 289 (2005), p. 356.
6. O. Cugat *et al.* *IEEE Trans. Magn.*, vol. 30 (1994), p. 4602.
7. T.A. Witten and L.M.P Sander. *Phys. Rev. Lett.*, vol. 47 (1981), p. 1400.
8. T. Vicsek. *Fractal growth phenomena* (World Scientific, 1989).
9. P. Meakin. *Fractals, scaling and growth far from equilibrium* (Cambridge University Press, 1998).